NASA Contractor Report 181984

ICASE Report No. 90–10

ICASE

TRIANGLE BASED TVD SCHEMES FOR HYPERBOLIC CONSERVATION LAWS

Louis J. Durlofsky
Stanley Osher
Bjorn Engquist

Contract No. NAS1–18605
January 1990

Institute for Computer Applications in Science and Engineering
NASA Langley Research Center
Hampton, Virginia 23665–5225

Operated by the Universities Space Research Association

National Aeronautics and
Space Administration

Langley Research Center
Hampton, Virginia 23665-5225

TRIANGLE BASED TVD SCHEMES FOR HYPERBOLIC CONSERVATION LAWS

Louis J. Durlofsky
Chevron Oil Field Research Company
P.O. Box 446
La Habra, CA 90633-0446

Stanley Osher[1,2] and Bjorn Engquist[2]
Department of Mathematics
UCLA
Los Angeles, CA 90024

ABSTRACT

A triangle based TVD (total variation diminishing) scheme for the numerical approximation of hyperbolic conservation laws in two space dimensions is constructed. The novelty of the scheme lies in the nature of the preprocessing of the cell averaged data, which is accomplished via a nearest neighbor linear interpolation followed by a slope limiting procedure. Two such limiting procedures are suggested. The resulting method is considerably more simple than other triangle based non-oscillatory approximations which, like this scheme, approximate the flux up to second order accuracy. Numerical results for linear advection and Burgers' equation are presented.

[1]This research was supported by the National Aeronautics and Space Administration under NASA Contract No. NAS1-18605 while the second author was in residence at the Institute for Computer Applications in Science and Engineering (ICASE), NASA Langley Research Center, Hampton, VA 23665.

[2]Research supported by Chevron Oil Field Research Company, ONR Grant N00014-86-K-0691, NSF Grant DMS 88-11863, DARPA Grant in the ACMP program, and NASA Langley Grant NAG1-270 and NASA University Consortium NCA-2372.

1. Introduction

In the last ten years there has been considerable effort aimed at constructing and analyzing high order accurate, non-oscillatory approximations to hyperbolic conservation laws (see *e.g.*, [2], [8]). It is by now well established that the spontaneous development of shock waves and the appearance of steep gradients in the solution require higher order schemes to have an adaptive stencil (by adaptive stencil we mean an adaptive flux approximation, *not* an adaptive grid) in order to suppress the spurious oscillations that plague conventional finite difference methods. Total variation diminishing (TVD) schemes, one such class of second order accurate methods that eliminate unphysical oscillations, have been used successfully in a variety of applications. Recently, a new class of methods, essentially non-oscillatory (ENO) schemes ([3], [4]), which surpass the second order accurate barrier associated with TVD schemes, has been developed. An alternative approach for third order schemes was developed in [10].

Extensions of TVD and ENO schemes to two and three dimensions are typically accomplished in a dimension by dimension fashion, via space-operator splitting. Therefore, the extension of these higher order schemes to the solution of hyperbolic conservation laws on unstructured grids, such as a triangular mesh, is not immediate. It is our intent in this paper to devise a second order accurate scheme of TVD type which is applicable to an unstructured triangular grid. Our scheme is based on a finite volume type discretization and is particularly straightforward to implement. The scheme relies on a very local adaptive interpolation idea, which results in computational efficiency. In the future, we expect to extend the adaptive two dimensional interpolation ideas presented here to develop triangle based, higher order ENO schemes.

Several approaches for the solution of hyperbolic conservation laws on triangular grids already exist. These techniques are, however, in the context of finite element methods and have utilized flux corrected transport (FCT) ideas [6] or have required the generation of a complex auxiliary grid [9] or are truly finite element

methods in space and time and thus are more costly computationally [5]. The methodology presented here is, in our opinion, simpler and more efficient, primarily because a finite volume rather than a finite element approach is used, thus avoiding the overhead associated with finite element schemes.

The TVD, second order accurate methods we shall develop in §2 are technically neither total variation diminishing nor strictly second order accurate. We follow the convention of calling two dimensional schemes TVD if they are formal extensions of one dimensional TVD schemes, as our scheme is. In general, however, the total variation may increase [1], though a maximum principle is satisfied. Also, although the fluxes are approximated up to second order, the truncation error is technically lower because of the adaptive stencil and the variable size of the triangles. Numerical experiments presented in §3 indicate orders of accuracy between 1.6 and 1.9 in the L_1 norm. In §4 we suggest further extensions of the method within the TVD context and indicate partial extensions to include diffusive terms.

2. Construction of the Numerical Schemes

Our intent in this section is to develop a scheme to solve hyperbolic conservation laws on triangular grids in two space dimensions. The method presented is for single hyperbolic conservation laws, though hyperbolic systems can be treated analogously in a field by field manner. Our method is finite volume based and achieves greater than first order accuracy through use of a novel adaptive flux interpolation procedure. We first present the general finite volume approach, then introduce our general limiting procedure, and then discuss various specific limiters.

2.1 Finite Volume Discretization

Consider the hyperbolic conservation law,

$$u_t + \nabla \cdot \mathbf{F}(u) = g(\mathbf{x}, t),$$

$$u(\mathbf{x},0) = u_0(\mathbf{x}), \tag{2.1}$$

subject to boundary conditions. We wish to solve (2.1) on a triangular grid, a portion of which is shown schematically in Fig. 1. Integrating (2.1) over a triangle (Δ_{ABC} to be specific) gives,

$$\frac{\partial}{\partial t}\int_{\Delta_{ABC}} u dA = -\int_{\Delta_{ABC}} (\nabla \cdot \mathbf{F}) dA, \tag{2.2}$$

where Δ_{ABC} represents both the region ABC and its area, and $g(\mathbf{x},t)$ has been taken to be zero for simplicity of exposition only. Applying the divergence theorem to the right hand side of (2.2) and defining,

$$\bar{u} = \Big(\int_{\Delta_{ABC}} u dA\Big)\big(\Delta_{ABC}\big)^{-1},$$

i.e., $\bar{u}$ is the average of u over Δ_{ABC}, gives,

$$\begin{aligned}\frac{\partial}{\partial t}\bar{u} = -\frac{1}{\Delta_{ABC}}\Big[&\int_{\ell_{AB}} \mathbf{F}\cdot\mathbf{n}_{AB} d\ell + \int_{\ell_{AC}} \mathbf{F}\cdot\mathbf{n}_{AC} d\ell, \\ &+ \int_{\ell_{BC}} \mathbf{F}\cdot\mathbf{n}_{BC} d\ell\Big].\end{aligned} \tag{2.3}$$

Note that $\bar{u}$ is equal to the value of u evaluated at the triangle centroid ($\mathbf{x}_{ABC}$) to within $O(\Delta_{ABC})$, or, analogously, to within $O(\ell^2)$, where ℓ is the characteristic length of a side of Δ_{ABC}. Here $\mathbf{n}$ is the unit outward normal.

We approximate (2.3) by first using a semi-discrete approach where the approximation is

$$v_{ABC}(t) \approx u_{ABC}(t);$$

the same is true for all triangles. First order accurate monotone schemes can easily be constructed - see *e.g.*, [7], [14]. Let $h_{BC}(w_1, w_2)$ be a two-point Lipschitz continuous monotone flux, approximating $\mathbf{F}\cdot\mathbf{n}_{BC}$, *i.e.*,

(2.4a) $h_{BC}(w,w) = \mathbf{F}\cdot\mathbf{n}_{BC}$,

(2.4b) $h_{BC}(w_1,w_2)$ is a nondecreasing function of w_1 and a nonincreasing function of w_2.

Then our semidiscrete monotone approximation is,

$$\frac{\partial}{\partial t}v_{ABC}(t) = -\frac{1}{\Delta_{ABC}}\Big[h_{BC}(v_{ABC}, v_{BCD})\cdot \ell_{BC} + h_{AB}(v_{ABC}, v_{ABF})\cdot \ell_{AB} + h_{AC}(v_{ABC}, v_{ACE})\cdot \ell_{AC}\Big], \tag{2.5}$$

where ℓ_{BC} is the length of the side BC, etc. "E" schemes may also be used - see [7] for the definition and for examples.

To obtain higher order accuracy we preprocess our initial data so that in each triangle, in particular Δ_{ABC}, a linear function is obtained whose cell average equals v_{ABC}, but which is within $O(\Delta)$ of u_{ABC} in regions of smoothness. Here Δ is the maximum area of the four triangles seen in Fig. 1. Moreover, this linear function will not introduce new oscillations in our approximation. This (simple) construction is the key part of this paper; it will be described at the end of this section. We call this linear approximation $L_\Delta(\mathbf{x})$. It is generally discontinuous across the boundary of each triangle.

Let $\mathbf{x}_{BC}$ be the midpoint of side BC, etc. Let $L_\Delta(\mathbf{x}^i_{BC})$ denote the limit of $L_\Delta(\mathbf{x})$ as $\mathbf{x} \to \mathbf{x}_{BC}$ from *inside* triangle ABC and $L_\Delta(\mathbf{x}^0_{BC})$ denote the limit as $\mathbf{x} \to \mathbf{x}_{BC}$ from *outside* triangle ABC. Generally,

$$|L_\Delta(\mathbf{x}^i_{BC}) - L_\Delta(\mathbf{x}^0_{BC})| = O(\Delta).$$

Our TVD, second order accurate, semi-discrete approximation to (2.3) is

$$\frac{\partial}{\partial t}v_{ABC}(t) = -\frac{1}{\Delta_{ABC}}\Big[h_{BC}(L_\Delta(\mathbf{x}^i_{BC}),\ L_\Delta(\mathbf{x}^0_{BC}))\cdot \ell_{BC} + h_{AB}(L_\Delta(\mathbf{x}^i_{AB}),\ L_\Delta(\mathbf{x}^0_{AB}))\cdot \ell_{AB} + h_{AC}(L_\Delta(\mathbf{x}^i_{AC}),\ L_\Delta(\mathbf{x}^0_{AC}))\cdot \ell_{AC}\Big]. \tag{2.6}$$

By the midpoint formula for integrals, this approximation is *weakly* second order accurate, in the sense that each of the three flux terms above is within $O(\Delta)$ of

the line integrals, $\int \mathbf{F} \cdot \mathbf{n} d\ell$, along the corresponding interfaces. However due to the shifting stencil and varying size and relation of the triangles, the pointwise truncation error is generally only $O(\Delta^{\frac{1}{2}})$, *i.e.*, first order. The performance appears to be around 1.6-1.9 order in L_1 for smooth flow (see §3).

2.2 Construction of Linear Function L_Δ

We now describe the construction of L_Δ. In each interior triangle, three candidates for L_Δ, designated L_Δ^i, are generated. The first such candidate L_Δ^1, is the linear interpolate of the three values

$$(\mathbf{x}_{ABC}, v_{ABC}),\ (\mathbf{x}_{BCD}, v_{BCD}),\ \ (\mathbf{x}_{ACE}, v_{ACE}),$$

L_Δ^2 is the interpolation of

$$(\mathbf{x}_{ABC}, v_{ABC}),\ \ (\mathbf{x}_{BCD}, v_{BCD}),\ \ (\mathbf{x}_{ABF}, v_{ABF}),$$

and L_Δ^3 the interpolation of

$$(\mathbf{x}_{ABC}, v_{ABC}),\ \ (\mathbf{x}_{ACE}, v_{ACE}),\ \ (\mathbf{x}_{ABF}, v_{ABF}).$$

These three linear interpolants are sketched in Fig. 2. Here and below we assume that the three triangle centroids, $\mathbf{x}_{ABC}, \mathbf{x}_{BCD}$ and $\mathbf{x}_{ABF}$ are not colinear. At this point, three possible L_Δ^i exist, and a limited version of L_Δ must be selected from these. To accomplish this, we first compute the magnitude of the gradient of each L_Δ^i; *i.e.*,

$$[(\frac{\partial}{\partial x_1} L_\Delta^i)^2 + (\frac{\partial}{\partial x_2} L_\Delta^i)^2]^{\frac{1}{2}} \equiv |\nabla L_\Delta^i|, \quad \text{for} \quad i = 1, 2, 3. \tag{2.7}$$

By analogy with limiting procedures in one space dimension ([13]), a valid, though very non-compressive limiter, corresponds to the selection of the L_Δ^i for which $|\nabla L_\Delta^i|$ is the minimum. This choice is analogous to the *min* limiter in second order ENO methods ([3]); no special precautions need be taken at extrema.

It is desirable to construct a more compressive limiter than that described above, particularly for problems involving linear or contact discontinuities. To accomplish this, we first consider the more compressive slope limiters in one dimension, the Φ type limiters described by Sweby [13] (his equation 3.17) of which superbee is the most compressive, corresponding to $\Phi = 2$. These limiters allow the use of piecewise linear approximations to the solution for which the slope is not the minimum, subject to the restriction that no overshoot (or undershoot) occurs at the cell boundaries.

The next limiter we describe is a multidimension analog of the one dimensional Φ limiters. The approach here is to select the L^i_Δ for which $|\nabla L^i_\Delta|$ is maximized, subject to the restriction that no overshoot or undershoot occurs at any of the three triangle boundaries. The procedure is as follows:

(i) Select the L^i_Δ for which $|\nabla L^i_\Delta|$ is the maximum.

(ii) Check for overshoot or undershoot at $\mathbf{x}_{AB}, \mathbf{x}_{AC}$ and $\mathbf{x}_{BC}$. For L^i_Δ to represent a valid L_Δ, it suffices to verify that, for Δ_{ABC},

$L_\Delta(\mathbf{x}_{AC})$ is between v_{ABC} and v_{ACE},

$L_\Delta(\mathbf{x}_{AB})$ is between v_{ABC} and v_{ABF} and

$L_\Delta(\mathbf{x}_{BC})$ is between v_{ABC} and v_{BCD}.

If these three requirements are satisfied, L^i_Δ is the appropriate L_Δ.

(iii) If the L^i_Δ above results in overshoot or undershoot at any one of the three midpoints, select the L^i_Δ for which $|\nabla L^i_\Delta|$ is the second largest and repeat the test in (ii). If this L^i_Δ does not satisfy the test in (ii), select the L^i_Δ for which $|\nabla L^i_\Delta|$ is the minimum and again proceed through the test in (ii).

(iv) If all L^i_Δ fail (ii), revert to a piecewise constant approximation for Δ_{ABC}; *i.e.*, $L_\Delta = v_{ABC}$.

Given L_Δ, the right hand side of (2.6) can be evaluated and $v_{ABC}(t)$ integrated in time. This time integration is accomplished via a second order TVD Runge-Kutta procedure [11].

3. Numerical Verification of Higher Order Scheme

In this section we present results for the convergence of the general method described in §2, as well as solution contours and profiles demonstrating the accuracy of the method. In all cases, the solution region is a square domain discretized via right triangular 'volumes' (referred to as elements), as shown in Fig. 3. Periodic boundary conditions are imposed in both the $x-$ and the $y-$ directions; the initial condition is similarly $x-$ and $y-$ periodic. In all cases the more compressive limiter described in §2.2 is used for the TVD scheme.

3.1 Rate of Convergence

To assess rate of convergence, the scheme is applied to the solution of the linear conservation law

$$u_t + \nabla \cdot (\mathbf{a}u) = 0, \tag{3.1}$$

subject to the initial condition

$$u_0(x, y) = \sin(2\pi x)\sin(2\pi y). \tag{3.2}$$

Our base monotone scheme uses the EO flux [7]:

$$h(w_1, w_2) = f_+(w_1) + f_-(w_2). \tag{3.3}$$

For linear equations with constant $\mathbf{a} = (a_x, a_y)$,

$$f_+(u) = [\max((\mathbf{a} \cdot \mathbf{n}), 0)]u, \tag{3.4a}$$

$$f_-(u) = [\min((\mathbf{a} \cdot \mathbf{n}), 0)]u. \tag{3.4b}$$

For Burgers' equation (considered below), where $f_1 = f_2 = (1/2)u^2$,

$$f_+(u) = \max((\frac{n_x + n_y}{2})u^2, 0), \tag{3.5a}$$

$$f_-(u) = \min((\frac{n_x + n_y}{2})u^2, 0), \tag{3.5b}$$

where n_x and n_y represent the components of $\mathbf{n}$.

A contour plot of the initial condition (3.2) is shown in Fig. 4. Four extrema are evident. The rate of convergence of the method was determined for both the case $a_x = a_y = 1$ and $a_x = 1,\ a_y = 0$. Further, convergence was assessed both on an element by element basis and after applying a local averaging procedure. It is expected that local averaging procedures would enhance the rate of convergence, as the scheme is expected to be second order in only the weak sense; *i.e.*, after integrating locally in space and time (a type of local averaging). The averaging performed in this study is, however, only spatial; no temporal averaging is attempted. This is because spatial-temporal averages are rather cumbersome to perform in practice, and the spatial averaging alone reveals the expected trend. Computations were performed for grids ranging in discretization from 200 elements ($\ell = 0.1$, where ℓ is the spacing between adjacent nodes or, analogously, $\ell = (2\Delta)^{1/2}$, with Δ the area of any element) to 12800 elements ($\ell = 0.0125$). In all cases the CFL number, $\lambda(= \Delta t/\ell)$, was set to 0.1.

Displayed in Fig. 5 is a log-log plot of L_1 error versus ℓ. In this case, $a_x = a_y = 1$. Results are shown for both a first order scheme and the higher order scheme, with error computed on an element by element basis. Least squares linear fits give the order of convergence for the two methods; for the first order method we obtain 0.93 and for the higher order method 1.77. Figure 6 displays an analogous plot after applying a local averaging procedure. Specifically, this averaging procedure entails averaging the computed value of u over square regions comprised of two adjacent elements and computing the error in terms of the difference between this average and the exact solution of Eq. (3.1) evaluated at the square midpoint. For the grid displayed in Fig. 3, 100 such square regions exist. Again, averaging is only applied spatially; no temporal averaging is performed. Assessing error in this manner results in least squares linear fits of slope 0.94 for the first order method and 1.81 for the higher order method. As expected, local averaging enhances the rate of convergence though, in this case, the improvement is minimal. In other cases, however, the improvement is more substantial. For example, using $a_x = 1,\ a_y = 0$

in Eq. (3.1) yields the following convergence results. For the first order method, convergence is $O(0.99)$ with no local averaging and $O(1.06)$ with averaging. For the higher order scheme, the convergence rates are $O(1.60)$ and $O(1.73)$, respectively.

Results for L_2 and L_∞ error display slower rates of convergence. For the case $a_x = a_y = 1$, L_2 error is $\sim O(\ell^{1.64})$ with local averaging and $O(\ell^{1.62})$ on an element by element basis with L_∞ error $\sim O(\ell^{0.94})$ with local averaging and $O(\ell^{0.91})$ with no averaging. The expected result for L_2 error is $\sim O(\ell^{1.5})$ and for L_∞ error $\sim O(\ell)$, as in one dimensional TVD methods. Although the discrepancies between the expected and numerical results are relatively slight, it is not clear why the L_2 error converges faster than expected while the L_∞ error converges slower than expected.

Shown in Table 1 is a compilation of the rates of convergence of L_1, L_2 and L_∞ error. Results for both a first order scheme and our more compressive TVD scheme are displayed. In all cases the initial condition is as in (3.2). Error is computed over the entire domain in two ways: (1) element by element and (2) by combining two adjacent elements into squares. In all cases ℓ ranges from 0.0125 to 0.1.

Slightly improved rates of convergence in L_1 are obtained when the initial condition contains no extrema. This is demonstrated in Table 2, where results for L_1 error for the initial condition $u_0(x,y) = \sin(\pi x/2)\sin(\pi y/2)$ are displayed. Here, to eliminate the effects of the discontinuity in u at the boundary (recall that periodic boundary conditions are imposed), error is computed only over the region $0.6 \leq x, y \leq 0.8$ at an early time, $t = 0.05$. In one case, local averaging has a more dramatic effect, improving the L_1 accuracy of the TVD scheme from 1.22 to 1.80.

Based on the numerical results presented above and the analysis presented in §2, we feel that the method can be considered to be second order accurate in L_1 in the weak sense. Though our convergence results always indicate convergence slower than quadratic, this is, in our opinion, due to the fact that these results are not strictly measuring weak convergence. If such convergence could be unambiguously

measured, it is our contention that the method would indeed display second order convergence.

3.2 Examples of Numerical Accuracy

We now present some detailed numerical results for our second order scheme and compare these with the results of a first order method. The first results are for the solution of Eqs. (3.1) and (3.2) with $a_x = a_y = 1$. Figure 7 displays the solution contour results for the first order scheme with 800 elements ($\ell = 0.05$) and $\lambda = 0.1$ (the same CFL number is used in all computations) at $t = 1$. The exact solution is a reproduction of the initial condition, shown in Fig. 4. The first order method is clearly very diffusive; the maximum value of u is here only 0.25, in contrast to the maximum in the initial condition of 1. Results for the second order scheme at $t = 1$ are shown in Fig. 8. Though some distortion of the initial condition is apparent, the solution is considerably improved over the first order solution; the maximum value of u is now 0.76. Shown in Fig. 9 are the $t = 1$ results for the first order scheme using 3200 elements ($\ell = 0.025$). Substantial numerical diffusion is still evident; the maximum value of u is only 0.49. The solution contour using the second order method is displayed in Fig. 10. The $t = 1$ solution in this case closely resembles the initial condition, with a maximum value of u of 0.88. Figures 11 and 12 show solution profiles taken along the line $y = x$ (the velocity direction) at $t = 0,\ 0.25,\ 0.5,\ 0.75$ and 1 for both the first and second order methods. In both cases, 3200 elements were used. The second order results are quite sharp at all times, while the first order results show a continual degradation with increasing time.

Solution profiles for computations using the second order method with a non-linear flux function, $f = (1/2)u^2$ in Eq. (2.1) (*i.e.*, the inviscid Burgers' equation), with the initial condition $u_0(x, y) = \sin(2\pi x)$, are shown in Fig. 13. Though this is an essentially one dimensional problem, no overshoot or unphysical oscillations appear in the solution. The solution is sharper with the second order method than

with a first order scheme (first order results are not shown), though the improvement is of course less dramatic than in the linear examples presented above.

4. Possible Extensions

Other limiting procedures are quite feasible and should be tested. Our compressive limiter is not a direct analogue of superbee, since superbee (and many other limiters [13]) occasionally allows values other than zero or any of the slopes being compared to be the final choice of slope (or gradient in our two dimensional case).

A more significant issue is the treatment of diffusive terms. In this case, the governing equation is of the form

$$u_t + \nabla \cdot \mathbf{F}(u) = \epsilon(u_{xx} + u_{yy}), \quad \epsilon > 0. \tag{4.1}$$

The discrete analogue of (2.3) now involves the additional term,

$$\frac{\epsilon}{\Delta_{ABC}}\left(\int_{\ell_{AB}} \frac{\partial u}{\partial n} d\ell + \int_{\ell_{AC}} \frac{\partial u}{\partial n} d\ell + \int_{\ell_{BC}} \frac{\partial u}{\partial n} d\ell\right), \tag{4.2}$$

on the right side of (2.3). Up to first order accuracy, we compute each of the three terms in (4.2) as follows. The limiting procedure has already given us a gradient within the triangle ABC as well as for each of the three neighbors. Therefore, the integral along side AB in (4.2) can be computed approximately as

$$[(\nabla L_{ABC} + \nabla L_{ABF}) \cdot \mathbf{n}]\frac{\ell_{AB}}{2}. \tag{4.3}$$

The integrals along the other sides are approximated analogously. This is generally a first order accurate method (second order accuracy occurs in special cases; *e.g.*, if all the triangles are equilateral). However, since ϵ is relatively small here (otherwise transport is diffusion dominated and the sophisticated treatment of convection is unnecessary), we believe this to be an adequate treatment of these terms.

Finally, we mention that work is underway to approximate (2.1) using a higher order accurate ENO triangle based method. See [11], [12] for successful Cartesian coordinate approaches.

References

[1] Goodman, J.B. and LeVeque, R.J., On the accuracy of TVD schemes in two space dimensions, *Math. Comp.*, **45**, 15-21, (1985).

[2] Harten, A., On the nonlinearity of modern shock-capturing schemes, in *MSRI Publ.*, **7**, 147-201, A. Chorin and A. Majda, eds., Springer-Verlag, (1987).

[3] Harten, A., Osher, S.J., Engquist, B., and Chakravarthy, S.R., Some results on uniformly high order accurate essentially non-oscillatory schemes, *J. Applied Num. Math.*, **2**, 347-377, (1986).

[4] Harten, A., Engquist, B., Osher, S.J., and Chakravarthy, S.R., Uniformly high order accurate essentially non-oscillatory schemes, III, *J. Comput. Phys.*, **71**, 231-303, (1987).

[5] Hughes, T.J.R. and Tezduyar, T., Finite element methods for first order hyperbolic systems with particular emphasis on the compressible Euler equations, *Comput. Methods Appl. Mech. Engrg.*, **45**, 217-284, (1984).

[6] Löhner, R., Morgan, K., Vahdati, M., Boris, J.P, and Book, D.L., FEM-FCT: Combining unstructured grids with high resolutions, *Comm. in Applied Numerical Methods*, **4**, 717-729, (1988).

[7] Osher, S.J., Riemann solvers, the entropy condition and difference approximations, *SIAM J. Numer. Anal.*, **21**, 217-235, (1984).

[8] Osher, S. and Sweby, P.K., Recent developments in the numerical solution of conservation laws, in *IMA Conference Series*, **9**, 681-700, A. Iserles and M.J.D. Powell, eds., Clarendon Press, (1987).

[9] Rostand, P., and Stoufflet, B., TVD schemes to compute compressible viscous flows on unstructured meshes, in *Notes on Numerical Fluid Mechanics*, **24**, 510-520, J. Ballmann and R. Jeltsch, eds., Vieweg, Weisbaden, (1988).

[10] Sanders, R., A third order variation nonexpansive difference scheme for a single nonlinear conservation law, *Math. Comp.*, **51**, 535-558, (1988).

[11] Shu, C.-W. and Osher, S.J., Efficient implementation of essentially non-oscillatory shock capturing schemes, *J. Comput. Phys.* **77**, 439-471, (1988).

[12] Shu, C.-W. and Osher, S.J., Efficient implementation of essentially non-oscillatory shock capturing schemes, II, *J. Comput. Phys.*, **83**, 32-78, (1989).

[13] Sweby, P.K., High resolution schemes using flux limiters for hyperbolic conservation laws, *SIAM J. Numer. Anal.*, **21**, 995-1011, (1984).

[14] Tadmor, E., Numerical viscosity and the entropy condition for conservative finite difference schemes, *Math. Comp.*, **43**, 369-382, (1984).

Table 1. Computed accuracy of TVD scheme for the linear case. Initial condition $u_0(x,y) = \sin(2\pi x)\ \sin(2\pi y)$. Error computed over the entire domain.

$$a_x = a_y = 1$$

Scheme	Norm	# elements	n
2nd O	L_1	1	1.77
2nd O	L_1	2	1.81
2nd O	L_2	1	1.62
2nd O	L_2	2	1.64
2nd O	L_∞	1	0.91
2nd O	L_∞	2	0.94
1st O	L_1	1	0.93
1st O	L_1	2	0.94
1st O	L_2	1	0.94
1st O	L_2	2	0.94
1st O	L_∞	1	0.95
1st O	L_∞	2	0.94

$$a_x = 1,\ a_y = 0$$

Scheme	Norm	# elements	n
2nd O	L_1	1	1.60
2nd O	L_1	2	1.73
1st O	L_1	1	0.99
1st O	L_1	2	1.06

Table 2. Computed accuracy (L_1) of TVD scheme for the linear case. Initial condition $u_0(x,y) = \sin(\pi x/2)\ \sin(\pi y/2)$ contains no extrema. Error computed over $0.6 \leq x, y \leq 0.8$ at $t = 0.05$.

$$a_x = a_y = 1$$

Scheme	# elements	n
2nd O	1	1.85
2nd O	2	1.87

$$a_x = 0,\ a_y = 1$$

Scheme	# elements	n
2nd O	1	1.22
2nd O	2	1.80
1st O	1	0.99
1st O	2	1.10

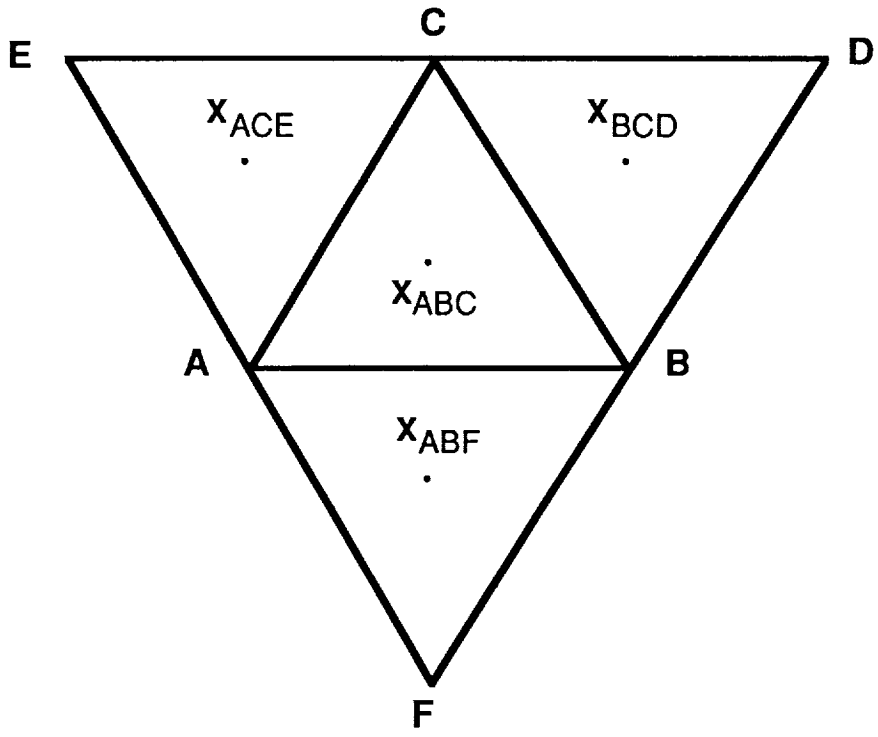

Figure 1

Schematic of a portion of the triangular grid.

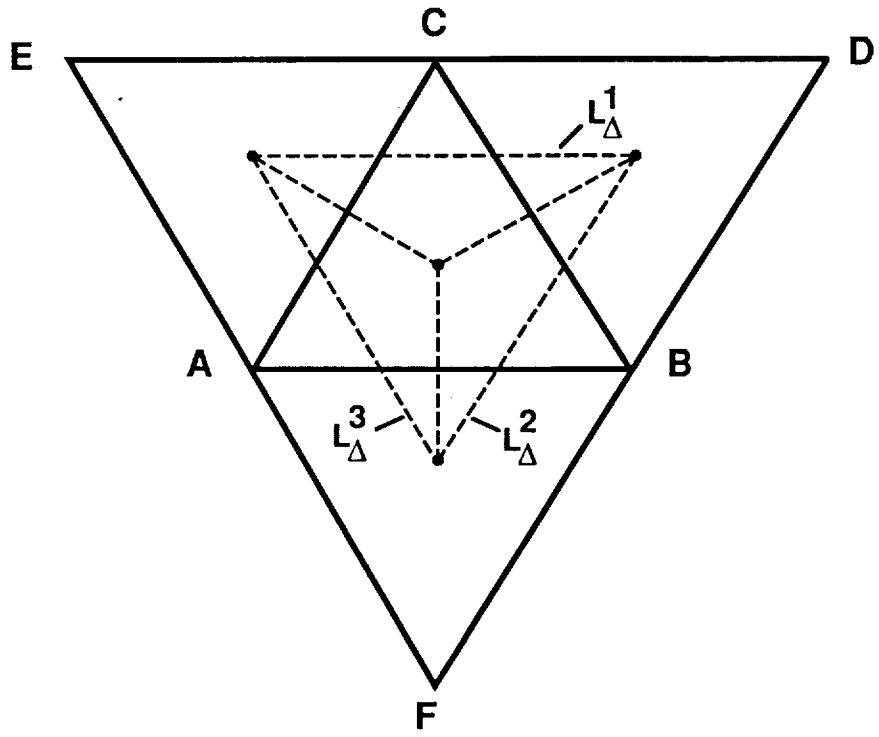

Figure 2

Three candidates for the linear interpolation of v over Δ_{ABC}.

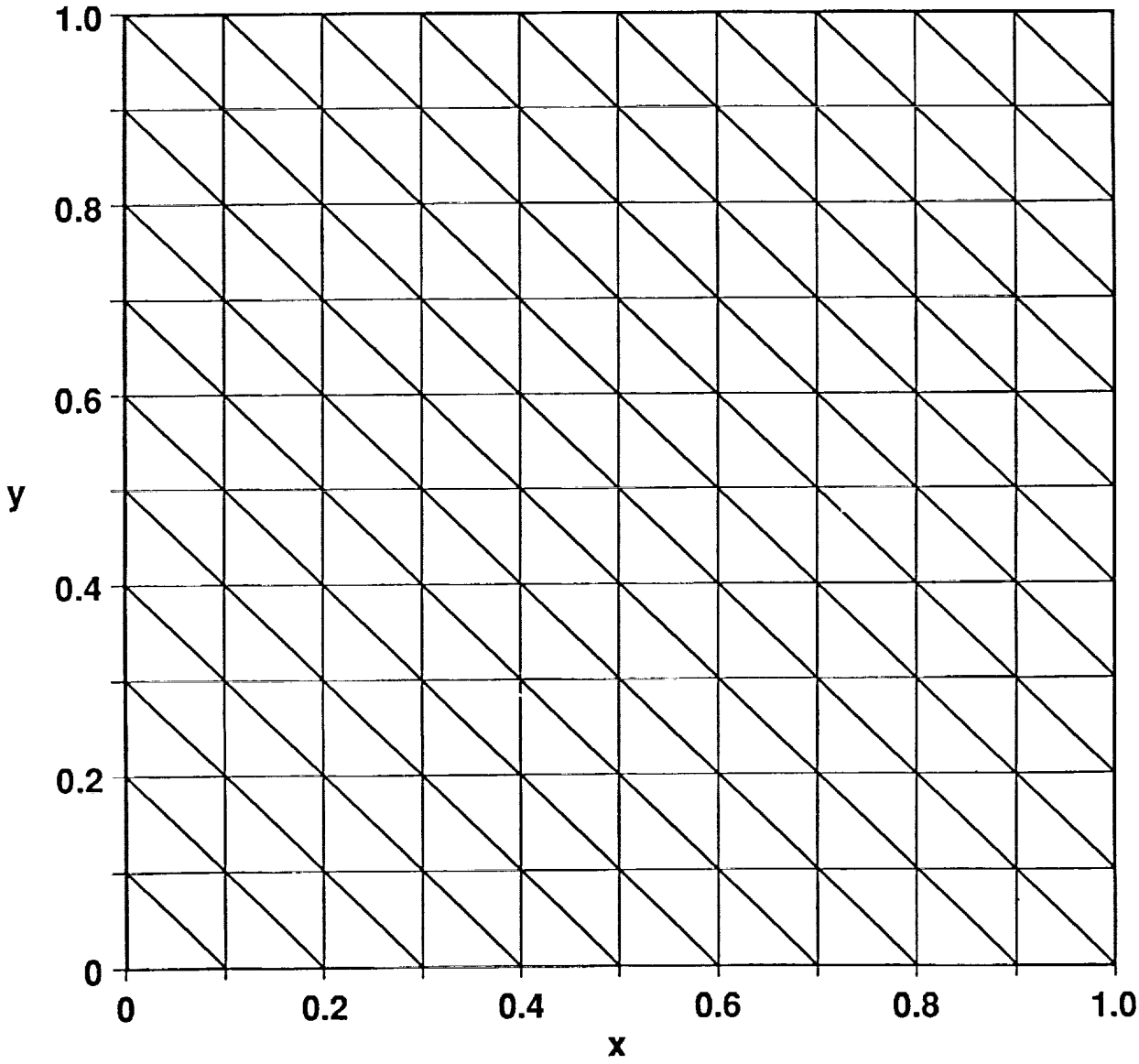

Figure 3

Triangular grid used for the numerical calculations.

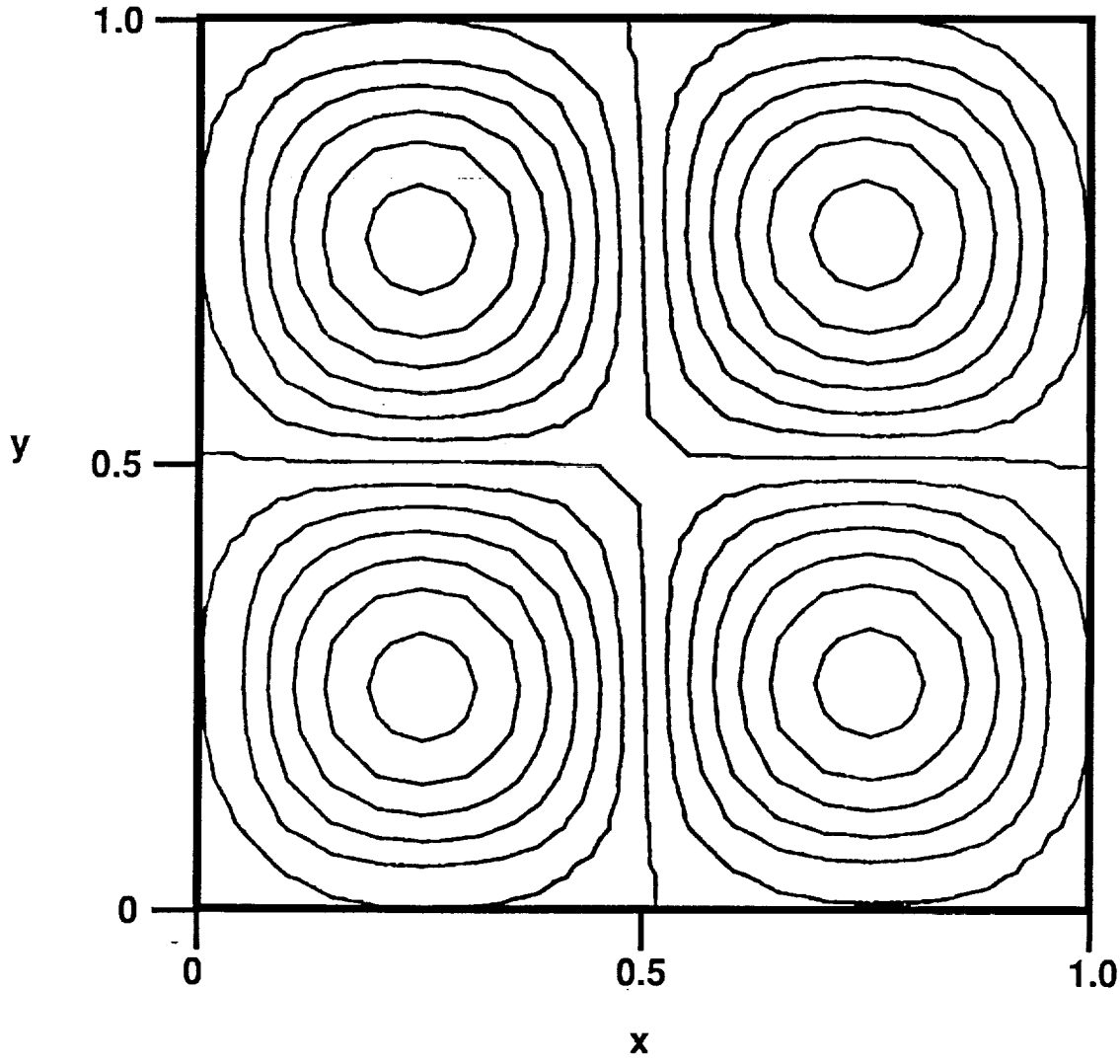

Figure 4

Contour plot of the initial condition (3.2). Contours correspond to u = 0, $\pm$ 0.15, $\pm$ 0.3, $\pm$ 0.45, $\pm$ 0.6, $\pm$ 0.75, $\pm$ 0.9.

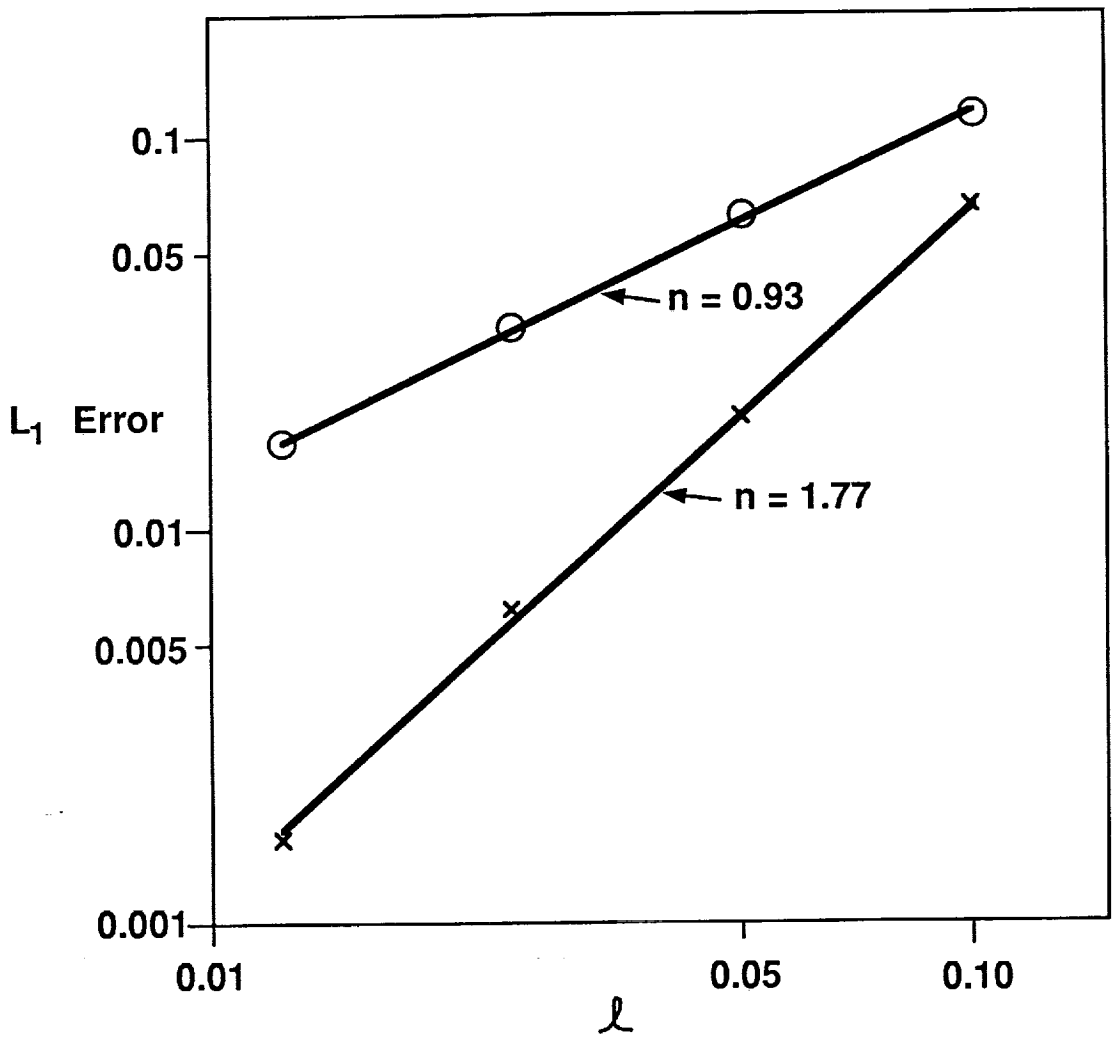

Figure 5

L_1 error on a per element basis for the case $a_x = a_y = 1$ for first order (○) and second order (×) schemes. Lines are least square fits with slopes as indicated.

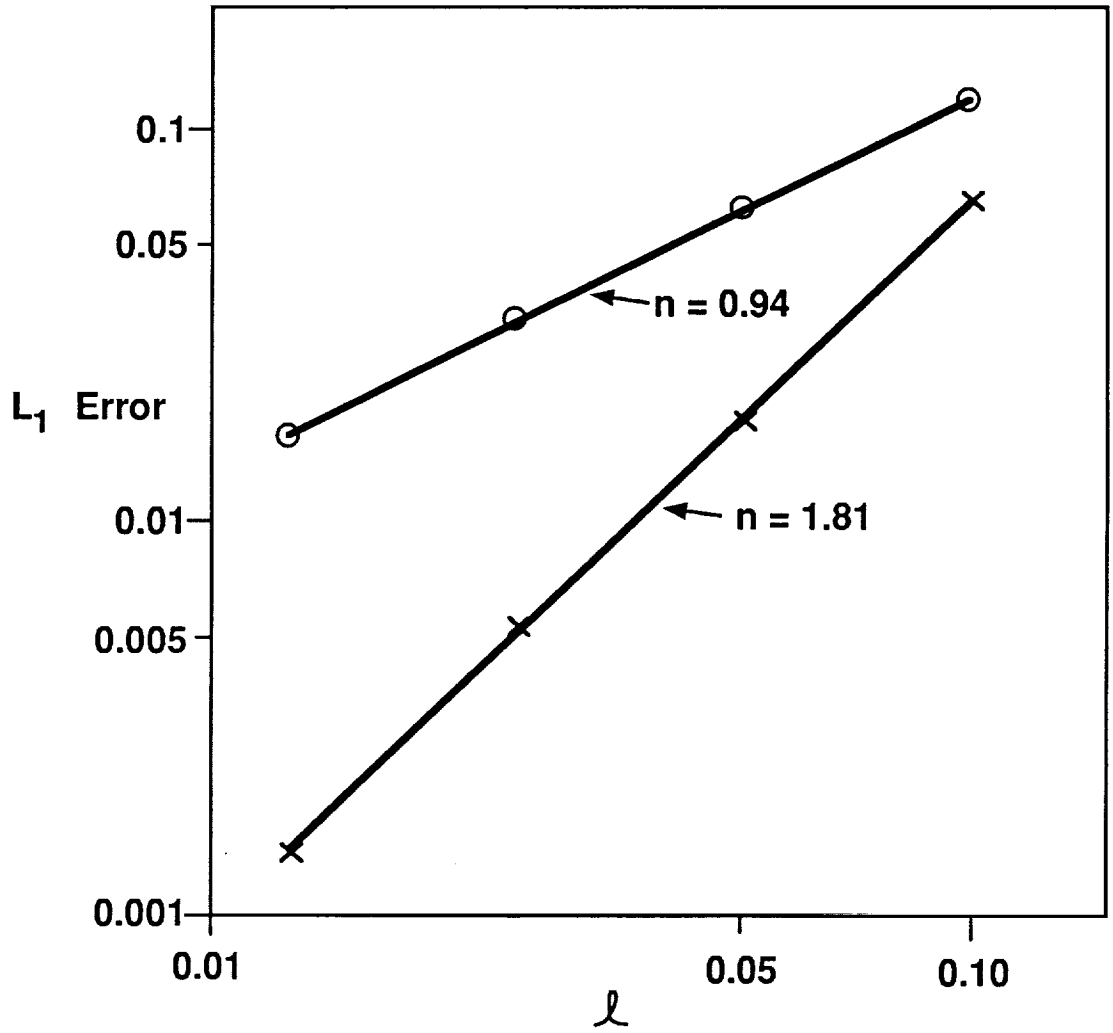

Figure 6

L_1 error after local averaging for the case $a_x = a_y = 1$ for first order (○) and second order (×) schemes. Lines are least square fits with slopes as indicated.

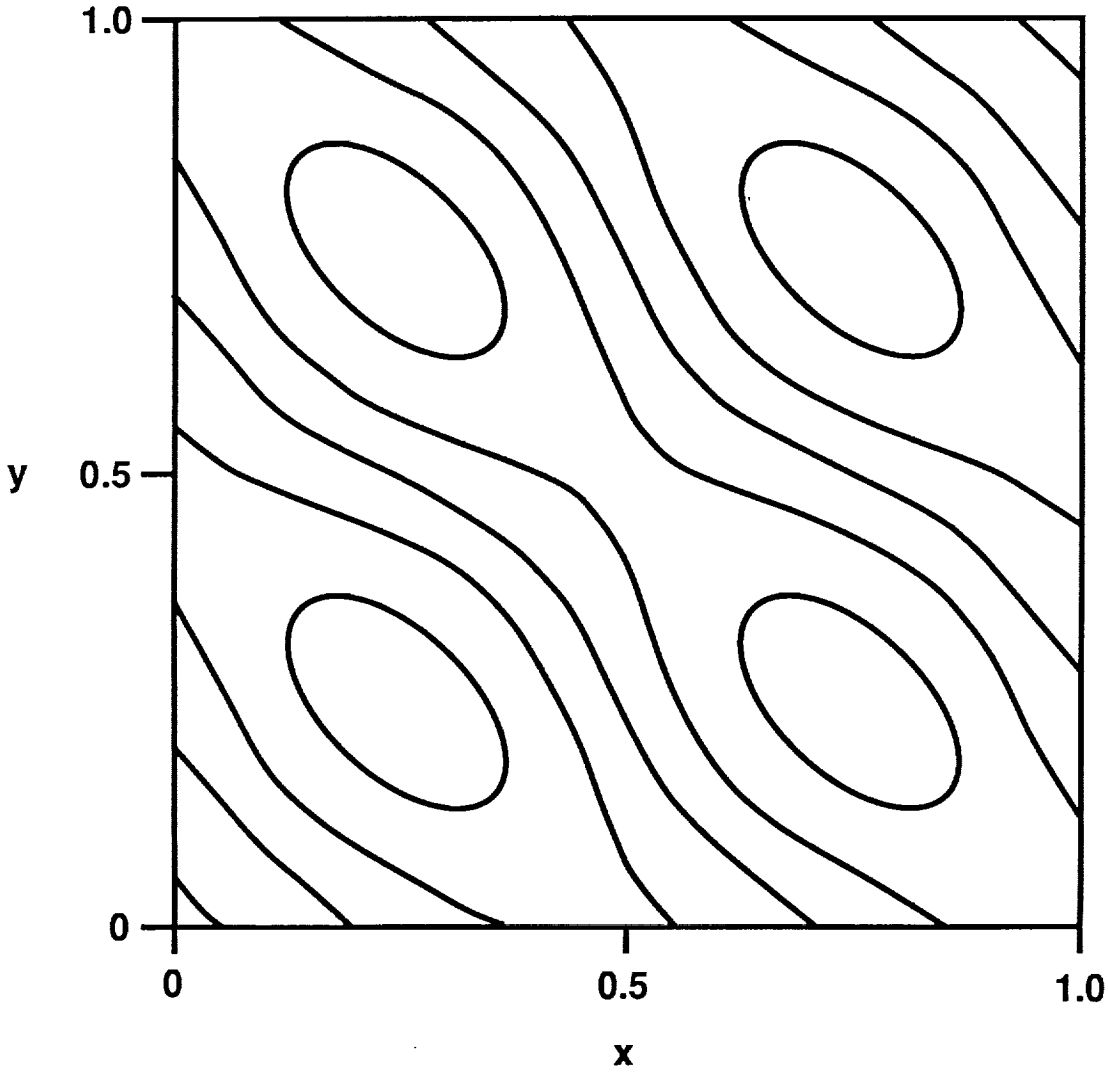

Figure 7

Results for first order scheme with 800 elements at t = 1.
Contours correspond to u = 0, $\pm$ 0.1, $\pm$ 0.2.

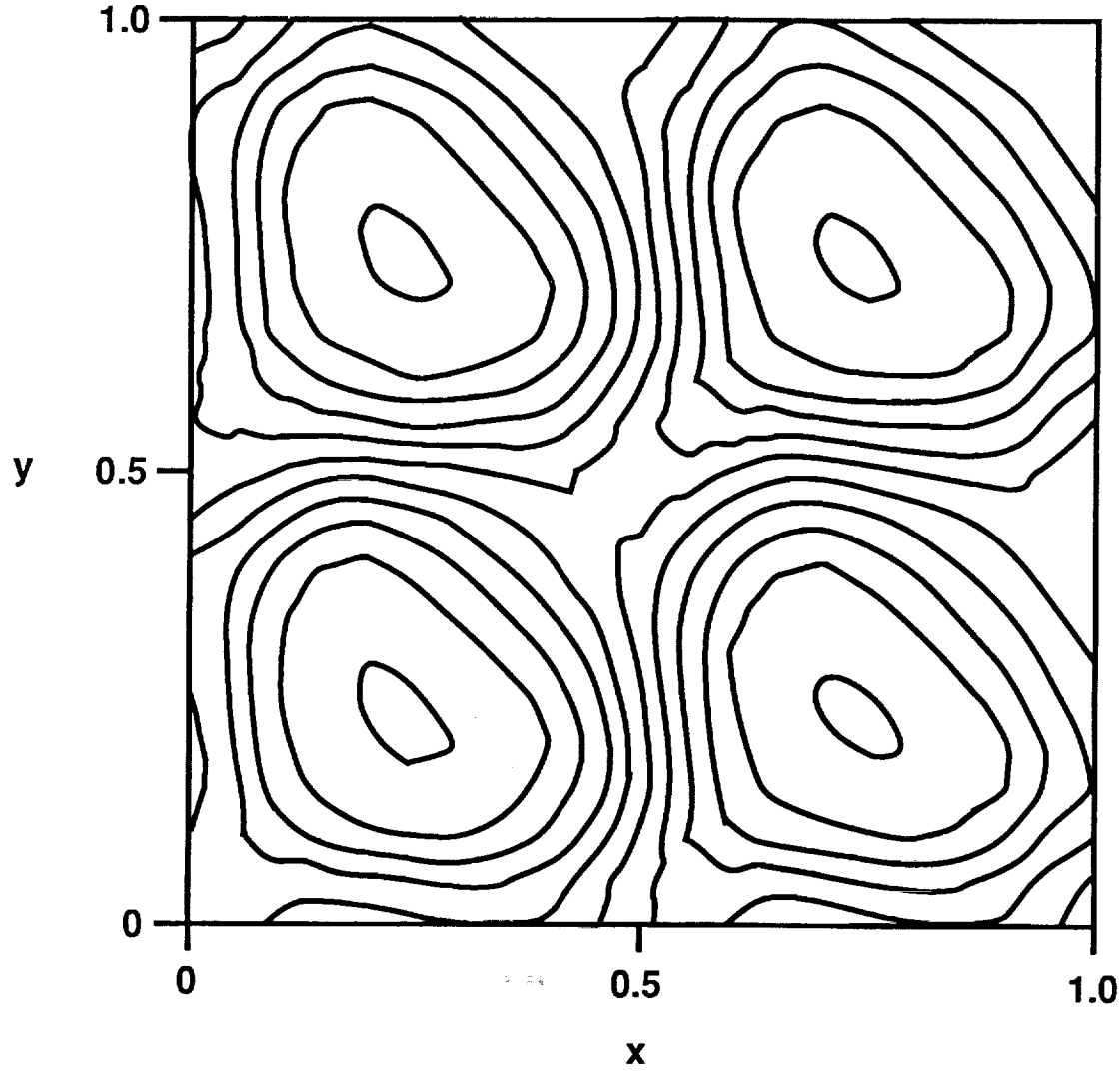

Figure 8

Results for second order scheme with 800 elements at t = 1. Contours correspond to u = 0, ± 0.15, ±0.3, ±0.45, ±0.6, ±0.75.

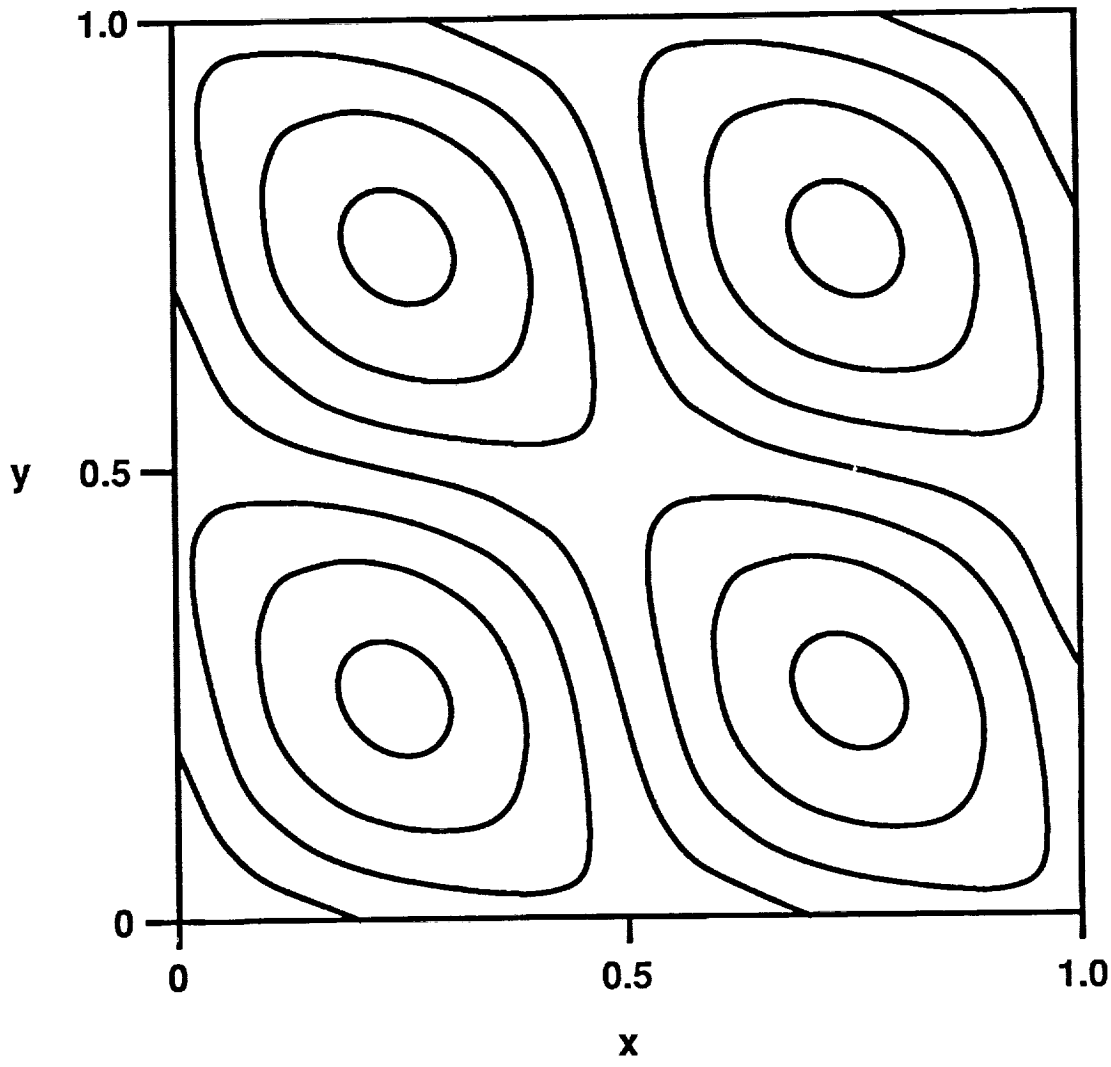

Figure 9

Results for first order scheme with 3200 elements at t = 1.
Contours correspond to u = 0, ± 0.15, ±0.3, ±0.45.

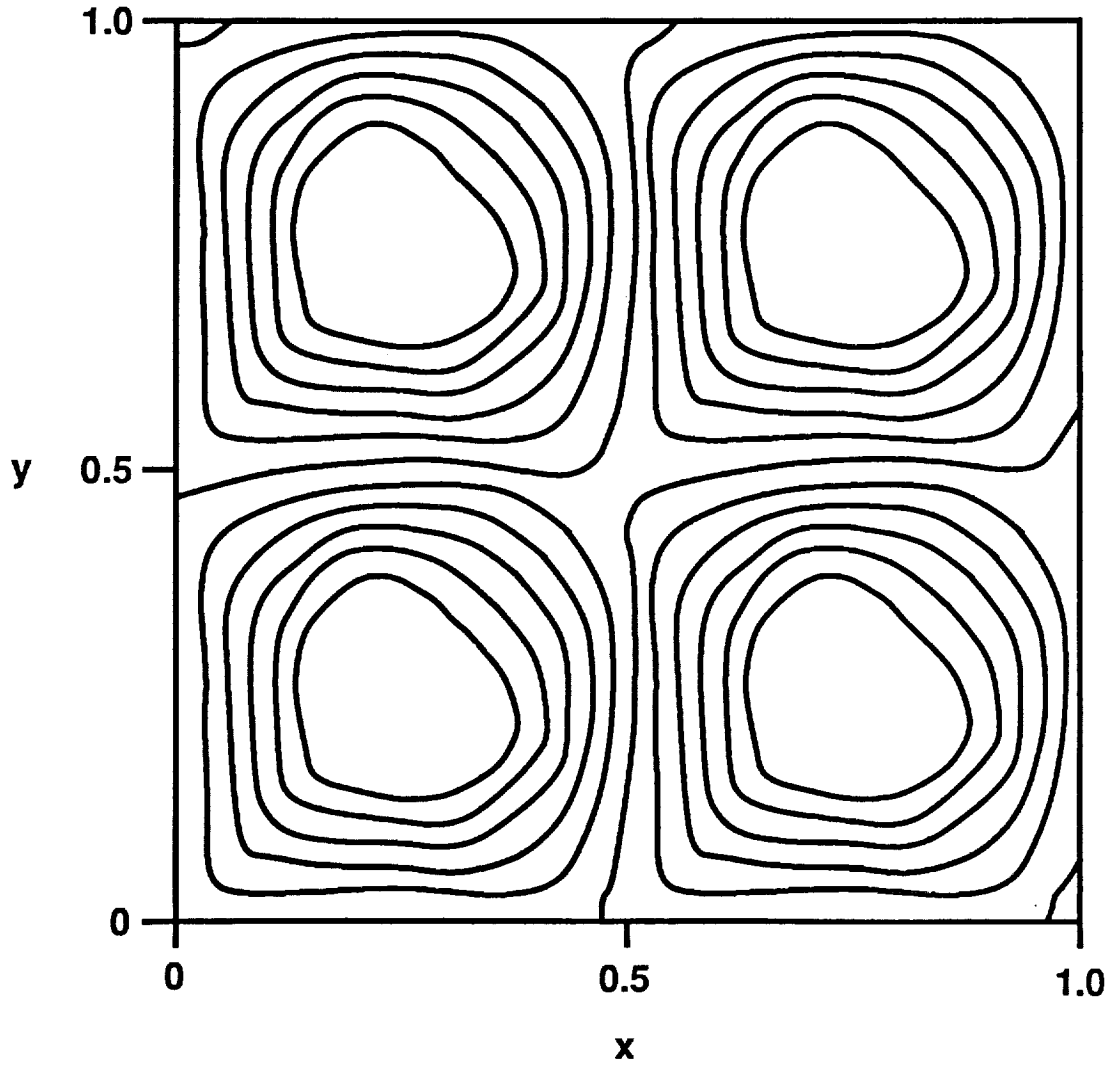

Figure 10

Results for second order scheme with 3200 elements at t =1.
Contours correspond to u = 0, ±0.15, ±0.3, ±0.45, ±0.6, ±0.75.

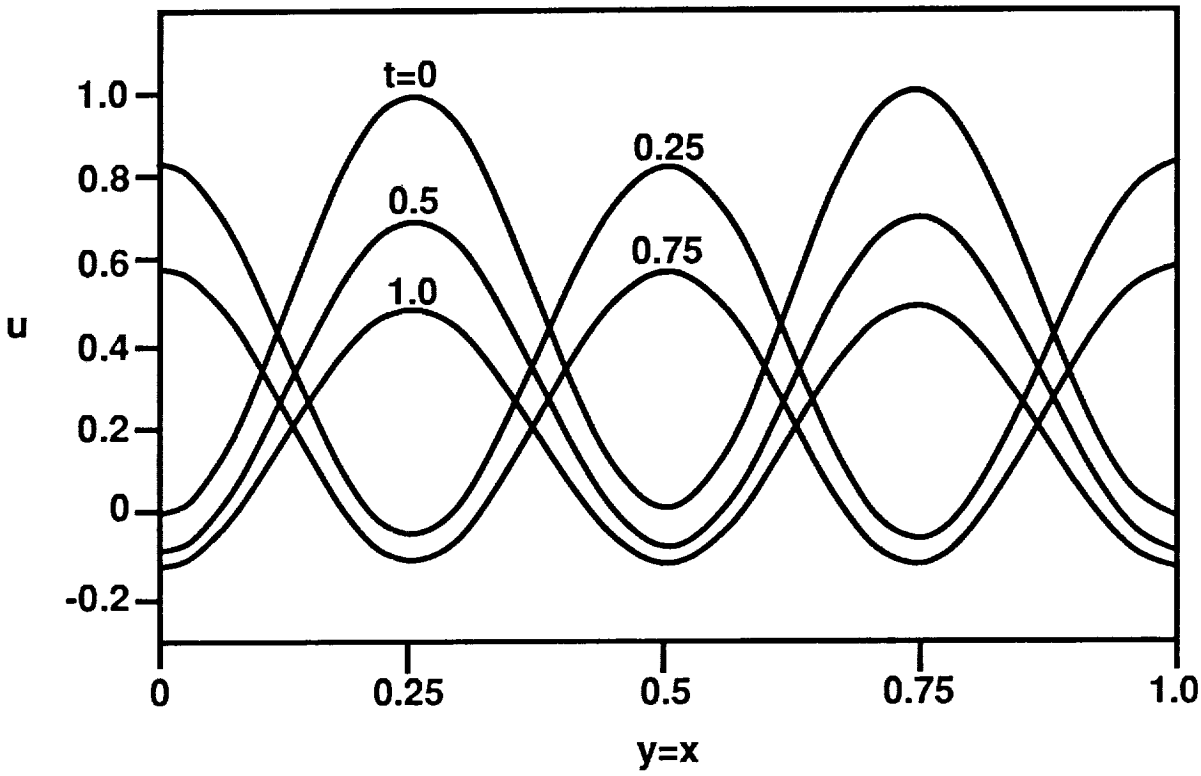

Figure 11

Solution profiles along the line y=x for the first order scheme (3200 elements).

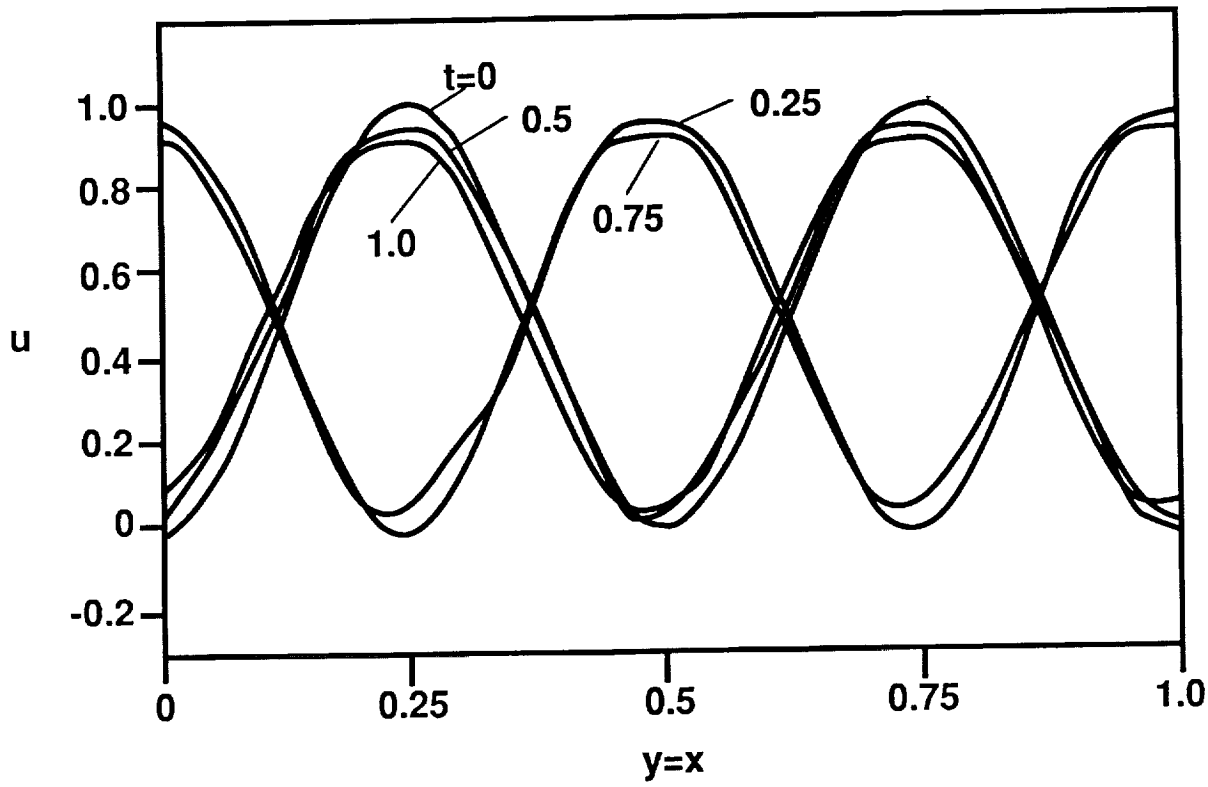

Figure 12

Solution profiles along the line y=x for the second order scheme (3200 elements).

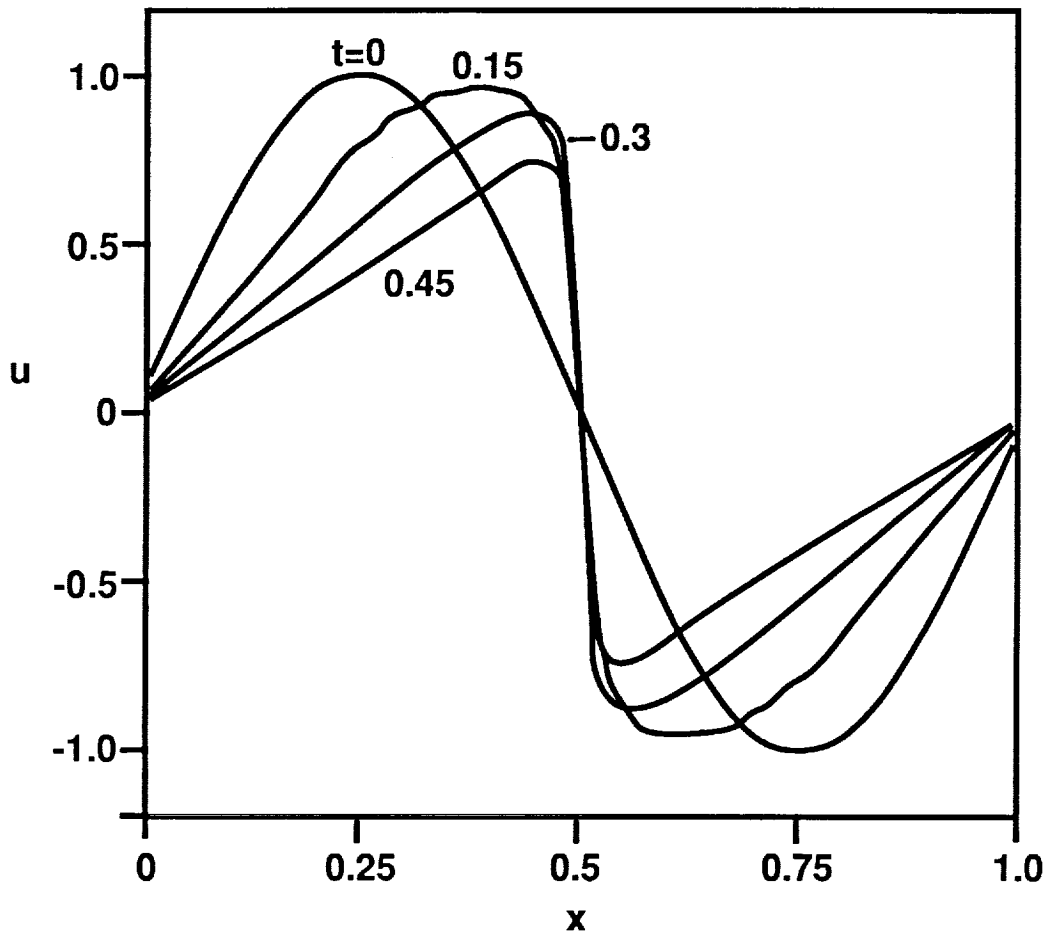

Figure 13

Solution profiles for Burgers' equation using second order scheme (800 elements).

NASA
National Aeronautics and Space Administration

Report Documentation Page

1. Report No.	2. Government Accession No.	3. Recipient's Catalog No.
NASA CR-181984 ICASE Report No. 90-10		

4. Title and Subtitle

TRIANGLE BASED TVD SCHEMES FOR HYPERBOLIC CONSERVATION LAWS

5. Report Date

January 1990

6. Performing Organization Code

7. Author(s)

Louis J. Durlofsky
Stanley Osher
Bjorn Engquist

8. Performing Organization Report No.

90-10

10. Work Unit No.

505-90-21-01

9. Performing Organization Name and Address

Institute for Computer Applications in Science and Engineering
Mail Stop 132C, NASA Langley Research Center
Hampton, VA 23665-5225

11. Contract or Grant No.

NAS1-18605

13. Type of Report and Period Covered

Contractor Report

12. Sponsoring Agency Name and Address

National Aeronautics and Space Administration
Langley Research Center
Hampton, VA 23665-5225

14. Sponsoring Agency Code

15. Supplementary Notes

Langley Technical Monitor:
Richard W. Barnwell

Final Report

Submitted to Journal of Computational Physics

16. Abstract

A triangle based TVD (total variation diminishing) scheme for the numerical approximation of hyperbolic conservation laws in two space dimensions is constructed. The novelty of the scheme lies in the nature of the preprocessing of the cell averaged data, which is accomplished via a nearest neighbor linear interpolation followed by a slope limiting procedure. Two such limiting procedures are suggested. The resulting method is considerably more simple than other triangle based non-oscillatory approximations which, like this scheme, approximate the flux up to second order accuracy. Numerical results for linear advection and Burgers' equation are presented.

17. Key Words (Suggested by Author(s))	18. Distribution Statement
TVD triangles, Hyperbolic Conservation Laws, limiters, triangular threads	59 - Mathematical and Computer Science (General) 64 - Numerical Analysis Unclassified - Unlimited

19. Security Classif. (of this report)	20. Security Classif. (of this page)	21. No. of pages	22. Price
Unclassified	Unclassified	30	A03

NASA FORM 1626 OCT 86